The Plant Cell, Vol. 17, 2981–2992, November 2005, www.plantcell.org

MYB98 Is Required for Pollen Tube Guidance and Synergid Cell Differentiation in *Arabidopsis* [W]

Ryushiro D. Kasahara,[1] Michael F. Portereiko,[1] Linda Sandaklie-Nikolova, David S. Rabiger, and Gary N. Drews[2]

Department of Biology, University of Utah, Salt Lake City, Utah 84112-0840

The synergid cells of the female gametophyte play a role in many steps of the angiosperm fertilization process, including guidance of pollen tube growth to the female gametophyte. However, the mechanisms by which the synergid cells become specified and develop their unique features during female gametophyte development are not understood. We identified *MYB98* in a screen for *Arabidopsis thaliana* genes expressed in the female gametophyte. *MYB98* is a member of the R2R3-MYB gene family, the members of which likely encode transcription factors. In the context of the ovule, *MYB98* is expressed exclusively in the synergid cells, and mutations in this gene affect the female gametophyte specifically. *myb98* female gametophytes are affected in two unique features of the synergid cell, pollen tube guidance and the filiform apparatus, but are otherwise normal. *MYB98* also is expressed in trichomes and endosperm. Homozygous *myb98* mutants exhibit no sporophytic defects, including trichome and endosperm defects. Together, these data suggest that *MYB98* controls the development of specific features within the synergid cell during female gametophyte development.

INTRODUCTION

The synergid cells within the female gametophyte (Figure 1A) are essential for the reproductive process in angiosperms. Sexual reproduction is initiated when the male gametophyte is transferred from the anther to the carpel's stigma, whereupon it forms a pollen tube that grows through the carpel's internal tissues to deliver its two sperm cells to the female gametophyte. The pollen tube enters the female gametophyte by growing into one of the two synergid cells. The synergid cell penetrated by the pollen tube typically undergoes cell death before or upon pollen tube arrival. Soon after arrival, the pollen tube ceases growth, ruptures, and releases its two sperm cells into the receptive synergid's cytoplasm, triggering the completion of degeneration. Finally, one sperm cell migrates to the egg cell and the other to the central cell to effect double fertilization of the female gametophyte (Weterings and Russell, 2004).

The synergid cells are required for pollen tube guidance. Using *Arabidopsis thaliana* mutants, several groups have shown that pollen tubes fail to grow onto ovules containing abnormal female gametophytes, suggesting that the embryo sac is the source of a pollen tube guidance cue (Hulskamp et al., 1995; Ray et al., 1997; Shimizu and Okada, 2000). Using laser ablation in an in vitro pollen germination system in *Torenia*, Higashiyama and colleagues (2001) showed that the synergid cells, but not other female gametophyte cells, are the source of the pollen tube attractant. Recently, a small maize (*Zea mays*) protein, EA1, required for pollen tube guidance was reported; however, maize EA1 is not likely to be a universal attractant because no homolog of *ea1* is present in *Arabidopsis* or other dicots (Marton et al., 2005).

The synergid cells also appear to control the late steps of the pollen tube growth pathway. In two *Arabidopsis* female gametophyte mutants, *feronia* (Huck et al., 2003) and *sirene* (Rotman et al., 2003), wild-type pollen tubes enter mutant female gametophytes but fail to cease growth, rupture, and release their contents. Similar pollen tube overgrowths occur in interspecific crosses of *Rhododendron* (Williams et al., 1986) and in the in vitro *Torenia* system (Higashiyama et al., 1998). These observations suggest that the female gametophyte contains factors that control the arrest of pollen tube growth and/or the release of pollen tube contents. Because these steps take place within the synergid cell, it is likely that synergid cell–expressed gene products are necessary for these processes (Weterings and Russell, 2004).

The synergid cells have several structural specializations that facilitate the fertilization process. At the micropylar pole, the cell wall is extensively invaginated, forming a structure referred to as the filiform apparatus (Figure 1B). The function of the filiform apparatus is unknown; numerous functions have been proposed, including pollen tube reception and transport of substances into and out of the synergid cells (Willemse and van Went, 1984; Huang and Russell, 1992). At the chalazal pole of the synergid cell, the cell wall is absent or discontinuous, which likely facilitates the fertilization process by providing direct access of the sperm cells to the fertilization targets (Willemse and van Went, 1984; Huang and Russell, 1992). Finally, during cell death, the synergid cytoskeleton reorganizes and forms two actin bands, which are thought to direct the migration of the sperm cells to the fertilization targets (Russell, 1993).

[1] These authors contributed equally to this work.

[2] To whom correspondence should be addressed. E-mail drews@bioscience.utah.edu; fax 801-581-4668.

The author responsible for distribution of materials integral to the findings presented in this article in accordance with the policy described in the Instructions for Authors (www.plantcell.org) is: Gary N. Drews (drews@bioscience.utah.edu).

[W] Online version contains Web-only data.

Article, publication date, and citation information can be found at www.plantcell.org/cgi/doi/10.1105/tpc.105.034603.

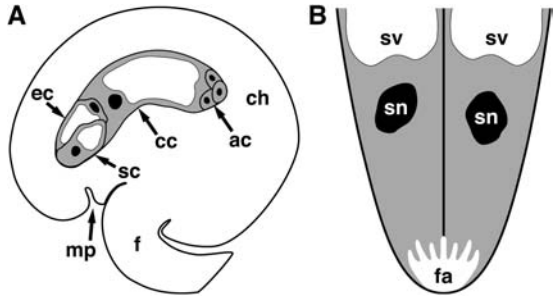

Figure 1. Depictions of the Female Gametophyte and Synergid Cells.

(A) Depiction of the *Arabidopsis* female gametophyte. Modified from Drews et al. (1998).

(B) Depiction of the synergid cells. This view is perpendicular to that in **(A)**.

The cytoplasm is gray, vacuoles are white, and nuclei are black. ac, three antipodal cells; cc, central cell; ch, chalazal region of the ovule; ec, egg cell; f, funiculus; fa, filiform apparatus; mp, micropyle; sc, synergid cell; sn, synergid cell nucleus; sv, synergid cell vacuole.

The molecular processes by which the synergid cells acquire their unique structure and function during cell differentiation are not understood. Regulatory molecules controlling these processes have not been identified. Furthermore, only a few genes expressed in synergid cells have been identified, and none of these is expressed exclusively in the synergid cells; these include the *Arabidopsis DEMETER* (Choi et al., 2002) and *AGP18* (Acosta-Garcia and Vielle-Calzada, 2004) genes and the maize *ea1* (Marton et al., 2005) and *es* (Cordts et al., 2001) genes.

Here, we report the identification of a gene, *MYB98*, that encodes an R2R3-type MYB protein, which likely functions as a transcription factor. In the context of the ovule, *MYB98* is expressed exclusively in the synergid cells. *MYB98* is required for pollen tube guidance and the formation of the filiform apparatus, both of which are unique features of the synergid cells. Thus, the *MYB98* gene appears to encode a regulatory molecule that controls synergid cell differentiation during female gametophyte development.

RESULTS

MYB98 Is Expressed in the Synergid Cells of the Female Gametophyte

We performed a screen to identify genes expressed in the female gametophyte. Our strategy was to identify mRNAs present in wild-type ovules but not in mutant ovules lacking female gametophytes. We used *determinant infertile1* (*dif1*) (Bai et al., 1999; Bhatt et al., 1999; Cai et al., 2003) as the source of mutant ovules. *dif1* ovules lack a female gametophyte but are otherwise normal; thus, genes exhibiting reduced expression in *dif1* ovules relative to wild-type ovules are likely to be expressed in the female gametophyte but not in the surrounding sporophytic tissue of the ovule.

To identify regulatory genes expressed in the female gametophyte, we harvested pistils from the wild type and *dif1*, extracted RNA, and used RT-PCR to assay the expression of genes within the R2R3-MYB family (Kranz et al., 2000; Stracke et al., 2001; Jiang et al., 2004). These genes likely encode transcription factors and have been shown to regulate many biological processes (Stracke et al., 2001; Jiang et al., 2004). These assays identified a gene, *MYB98*, exhibiting reduced expression in *dif1* pistils relative to wild-type pistils (Figure 2A).

To determine which cells within the female gametophyte express the *MYB98* gene, we generated and analyzed transgenic *Arabidopsis* plants containing Pro_{MYB98}:*reporter* constructs. As shown in Figures 3A and 3B, at the terminal developmental stage (stage FG7), Pro_{MYB98}:*green fluorescent protein* (*GFP*) and Pro_{MYB98}:β-*glucuronidase* (*GUS*) were expressed exclusively in the synergid cells. During the fertilization process, one of the synergid cells undergoes cell death and the other synergid cell persists. Expression was detected in the persistent synergid cell for ≥7 d after fertilization (Figure 3D).

To determine whether *MYB98* is expressed at earlier stages of female gametophyte development, we analyzed expression in flowers at stage 12c, which lack mature (stage FG7) female gametophytes (Christensen et al., 1997). Stage 12c flowers contained ~33% uncellularized (stages FG4 and early FG5) and

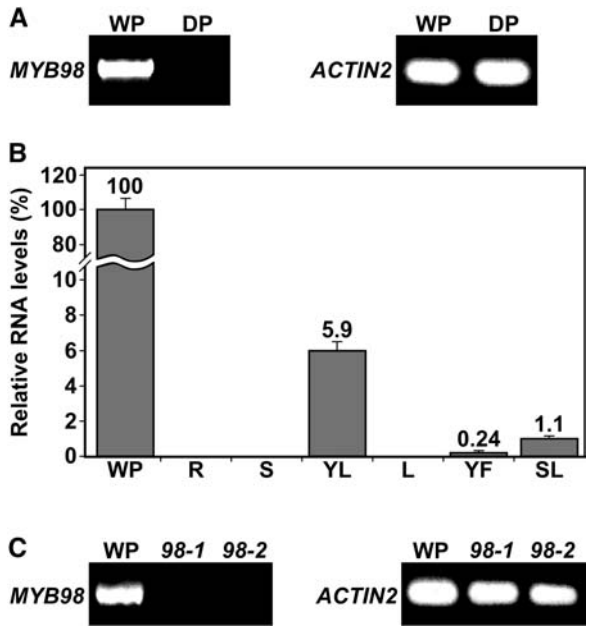

Figure 2. RT-PCR Analysis of *MYB98* Expression.

(A) Expression of *MYB98* in wild-type pistils (WP) and *dif1-2*/*dif1-2* pistils (DP). Expression of the *ACTIN2* gene was used as a control.

(B) Real-time RT-PCR analysis of *MYB98* expression in pistils (WP), roots (R), floral stems (S), young leaves at <5 mm in length (YL), older leaves at 10 to 20 mm in length (L), flowers at stages 1 to 11 (YF), and siliques at 1 to 2 d after pollination (SL). Each bar represents an average of four to five independent reactions. Error bars indicate SD. The number above each bar represents RNA level relative to pistil (WP).

(C) Expression of *MYB98* in wild-type pistils (WP), *myb98-1*/*myb98-1* pistils (*98-1*), and *myb98-2*/*myb98-2* pistils (*98-2*). Expression of the *ACTIN2* gene was used as a control.

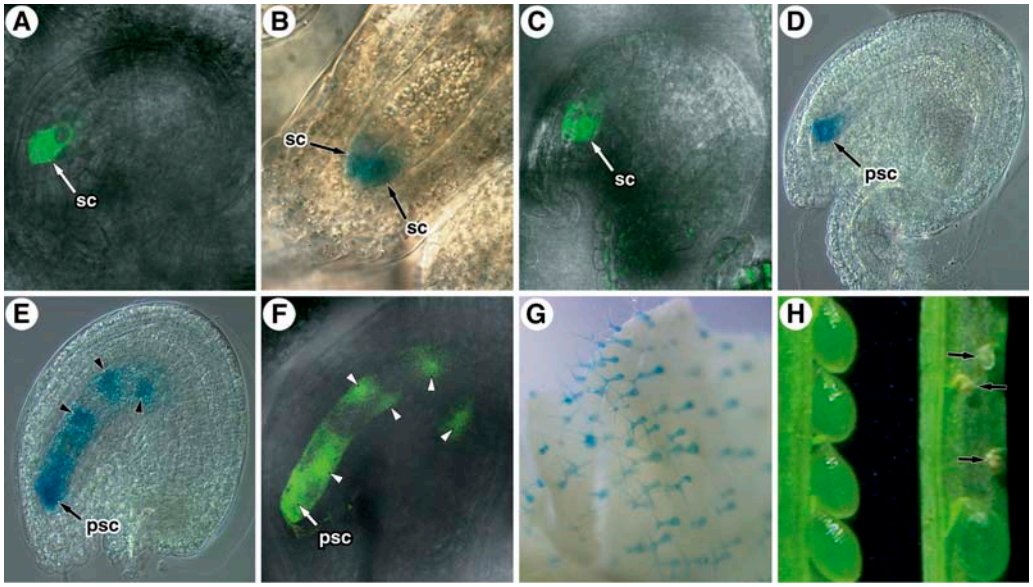

Figure 3. Expression of the Pro_{MYB98}:*GFP* and Pro_{MYB98}:*GUS* Genes.

(A) and **(B)** Expression of Pro_{MYB98}:*GFP* **(A)** and Pro_{MYB98}:*GUS* **(B)** in female gametophytes at the terminal developmental stage (stage FG7). Expression is detected only in the synergid cells. The ovule in **(A)** is oriented like that in Figure 1A, and the ovule in **(B)** is oriented like that in Figure 1B. The ovule in **(B)** was stained in 1 mM 5-bromo-4-chloro-3-indolyl-β-glucuronic acid (X-Gluc) for 30 min.

(C) Expression of Pro_{MYB98}:*GFP* in the synergid cells in a female gametophyte at late stage FG5.

(D) Expression of Pro_{MYB98}:*GUS* in a fertilized embryo sac at 12 h after pollination. Expression is detected only in the persistent synergid cell. This ovule was stained in 1 mM X-Gluc for 4 h.

(E) Expression of Pro_{MYB98}:*GUS* in a fertilized embryo sac at 12 h after pollination. Expression is detected in the persistent synergid cell and endosperm (arrowheads). This ovule was stained in 5 mM X-Gluc for 4 h.

(F) Expression of Pro_{MYB98}:*GFP* in a fertilized embryo sac at 24 h after pollination. Expression is detected in the persistent synergid cell and endosperm (arrowheads).

(G) Expression of Pro_{MYB98}:*GUS* in the trichomes of young (<5 mm) leaves. This leaf was stained in 1 mM X-Gluc for 16 h.

(H) Opened siliques from wild-type (left) and *myb98-1*/+ (right) plants at 10 d after pollination. Siliques from mutant plants contain desiccated ovules (arrows).

psc, persistent synergid cell; sc, synergid cell.

67% cellularized (stages late FG5 and FG6) female gametophytes ($n = 159$). In flowers at this stage, Pro_{MYB98}:*GFP* expression was detected in ~60% ($n = 200$) of the female gametophytes, in contrast with 100% of female gametophytes in mature ovules. All of the female gametophytes expressing Pro_{MYB98}:*GFP* had morphologically identifiable synergid cells (Figure 3C), indicating that cellularization had occurred. Together, these data suggest that *MYB98* is expressed in cellularized (late stage FG5 to FG7) but not uncellularized female gametophytes.

To determine whether *MYB98* is expressed elsewhere in the plant, we analyzed the Pro_{MYB98}:*reporter* lines and performed real-time RT-PCR with RNA from various organs. During seed development, Pro_{MYB98}:*GFP* and Pro_{MYB98}:*GUS* expression was detected only in the persistent synergid cell (Figure 3D) and the endosperm (Figures 3E and 3F). Expression in the endosperm was weak relative to that in the persistent synergid (cf. the staining conditions summarized in the legends of Figures 3D and 3E). During seed development, expression was highest in very young seeds (≤1 d after pollination) (Figures 3E and 3F) and diminished gradually at progressively older stages; expression was not detected in seeds older than 3 d after pollination.

Within vegetative organs, Pro_{MYB98}:*GUS* expression was detected only in the trichomes of leaves (Figure 3G). The leaf trichome expression was weak relative to the synergid expression (cf. the staining conditions summarized in the legends of Figures 3B and 3G). During leaf development, Pro_{MYB98}:*GUS* expression was highest in very young leaves (<5 mm in length) (Figure 3G) and diminished gradually at progressively older stages; expression was not detected in leaves longer than 8 mm. Within reproductive organs, strong Pro_{MYB98}:*GUS* expression was detected only in the synergid cells (Figure 3B); in addition, very weak expression was detected in the trichomes of sepals (data not shown).

Using real-time RT-PCR (Figure 2B), strong *MYB98* expression was detected only in pistils, which contain the synergid cells. In addition, weaker expression was detected in young leaves (<5 mm in length), which correlates with the expression of Pro_{MYB98}:*GUS* in the trichomes of young leaves (Figure 3G); in developing siliques, which correlates with the expression of Pro_{MYB98}:*GUS* in the persistent synergid cell (Figure 3D) and endosperm (Figure 3E); and in young flowers, which correlates with the expression of Pro_{MYB98}:*GUS* in the trichomes of sepals. Expression of *MYB98*

was not detected in roots, stems, and older leaves. Together, these data suggest that *MYB98* is expressed at high levels in the synergid cells and at lower levels in the endosperm of young seeds and the trichomes of young leaves and sepals.

MYB98 Gene Structure

To determine the structure of the *MYB98* gene, we isolated a *MYB98* cDNA clone and compared its sequence with the genomic sequence. As shown in Figure 4A, *MYB98* has three exons and two introns and is predicted to encode a protein of 427 amino acids. As shown in Figure 4B, MYB98 is predicted to contain a Myb domain (Kranz et al., 2000; Stracke et al., 2001) and a putative nuclear localization signal.

The Myb domain is a DNA binding motif found in the vertebrate protooncogene c-*myb* (Lipsick and Wang, 1999). The Myb domain in c-Myb consists of three imperfect tandem repeats (Myb repeats) of ~50 amino acids that are referred to as R1, R2, and R3. In c-Myb, R2 and R3 are required for sequence-specific binding and R1 is thought to play a minor role in DNA binding (Ogata et al., 1994). Structural studies of c-Myb have shown that each Myb repeat forms three α-helices, that the second and third α-helices form a helix-turn-helix structure, and that the third helices of R2 and R3 make direct contact with the major groove of the target DNA (Ogata et al., 1992, 1994, 1995).

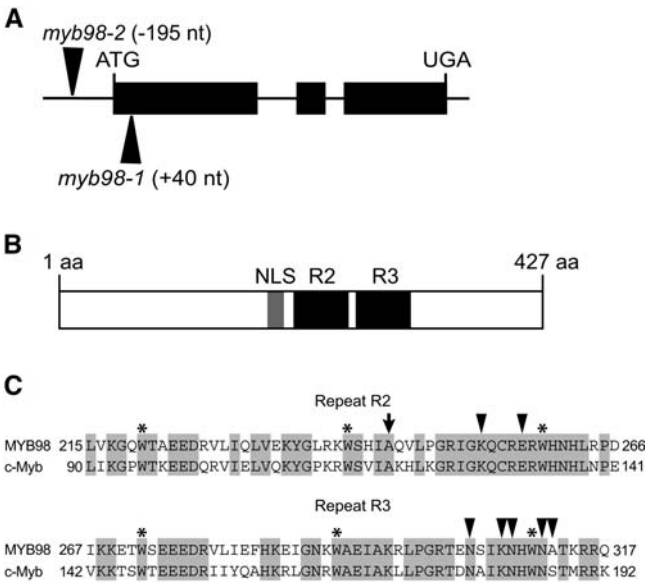

Figure 4. Structure of the MYB98 Protein.

(A) *MYB98* gene structure. Black boxes represent coding sequence, and arrowheads represent the T-DNA insertion sites in *myb98-1* (40 bp downstream of the ATG) and *myb98-2* (195 bp upstream of the ATG). nt, nucleotide.

(B) MYB98 protein structure. MYB98 contains a predicted nuclear localization signal (NLS) between amino acids (aa) 196 and 212 (gray box). The R2 and R3 repeats are represented by black boxes.

(C) Comparison of the R2 and R3 Myb repeats between *Arabidopsis* MYB98 and *Mus musculus* c-Myb. Conserved amino acids are shaded in gray. The asterisks denote the conserved Trp residues. The arrow designates the conserved Ala residue in the second helix of R2 that is often a Pro residue in plant R2R3 proteins (Jia et al., 2004). The arrowheads denote the seven amino acids in c-Myb that contact the DNA bases.

Most plant MYB proteins, including MYB98, contain only the R2 and R3 Myb repeats (Jin and Martin, 1999; Stracke et al., 2001; Jiang et al., 2004). The R2 and R3 Myb repeats of MYB98 are highly similar to those of c-Myb (66% identical and 86% similar at the amino acid level). The R2 and R3 Myb repeats of c-Myb contain six Trp residues that form the hydrophobic core of the helix-turn-helix structure (Kanei-Ishii et al., 1990) and seven amino acid residues that contact the DNA bases and contribute to DNA binding specificity (Tahirov et al., 2002) (Figure 4C). All of the Trp residues and six of the seven DNA-contacting residues are conserved in MYB98 (Figure 4C). Together, these observations suggest that MYB98 binds DNA and functions as a transcriptional regulator.

We also isolated a cDNA clone from the *Arabidopsis* Landsberg *erecta* accession and compared its sequence with that of the Columbia accession. This comparison revealed 16 nucleotide differences that are predicted to result in six amino acid differences (see Supplemental Figure 1 online). None of the amino acid differences are within the R2 and R3 Myb repeats, consistent with the predicted importance of these domains.

The *myb98* Mutation Affects the Female Gametophyte Specifically

To determine whether mutations in the *MYB98* gene affect the female gametophyte, we obtained lines containing T-DNA insertions in this gene from the Salk Institute Genomic Analysis Laboratory collection (Alonso et al., 2003). We analyzed two independent T-DNA alleles, *myb98-1* and *myb98-2*. The T-DNA in *myb98-1* is inserted into the first exon 42 nucleotides downstream of the start codon and 152 nucleotides upstream of the predicted R2 Myb repeat and is associated with a 23-bp deletion. The T-DNA in *myb98-2* is inserted into the genomic sequence 195 nucleotides upstream of the start codon and is associated with a 19-bp deletion. With both alleles, we did not detect wild-type *MYB98* transcripts by RT-PCR (Figure 2C), suggesting that they are null alleles.

With both alleles, siliques from heterozygous plants contained 50% desiccated ovules (Figure 3H), suggesting that these mutations cause gametophytic lethality. To determine whether the *myb98* mutations affect the female gametophyte, we crossed heterozygous mutant plants as female parents with wild-type males and scored the number of F1 progeny that were heterozygous and homozygous wild type. As summarized in Table 1, both alleles exhibited reduced transmission through the female gametophyte, indicating that the *myb98-1* and *myb98-2* mutations affect the female gametophyte.

To determine whether the *myb98* mutations also affect the male gametophyte, we crossed heterozygous mutant plants as male parents with wild-type females and scored the number of F1 progeny that were heterozygous and homozygous wild type. With both alleles, heterozygous and homozygous wild-type progeny were present in approximately equal proportions in

the F1 generation (Table 1), indicating that the *myb98-1* and *myb98-2* mutations do not affect the male gametophyte.

As shown in Table 1, plants homozygous for the *myb98-1* and *myb98-2* mutations were present among the progeny of self-pollinated plants. As expected, homozygous plants had dramatically reduced seed set, as a result of the female gametophyte defect; for example, *myb98-1/myb98-1* siliques contained an average of 83% desiccated ovules and 17% green seeds ($n = 15$ siliques) after self-pollination. Homozygous lines exhibited no sporophytic defects. In particular, homozygous mutants exhibited no overt trichome defects with regard to both density and branching. In addition, mutant siliques lacked abnormal seeds, suggesting that there were no defects in endosperm development. Together, these data indicate that the *myb98-1* and *myb98-2* mutations affect the female gametophyte specifically.

Molecular Complementation of the *myb98-1* Mutation

To determine whether the female gametophyte defect is attributable to disruption of the *MYB98* gene, we introduced a wild-type copy of the *MYB98* gene into the *myb98-1* mutant. We identified plants heterozygous for the *myb98-1* allele and hemizygous for the rescue construct and crossed these plants as females with wild-type males. In the F1 generation, *myb98-1/MYB98* and *MYB98/MYB98* progeny were present in a ratio of ~1:2. In addition, we identified plants homozygous for the *myb98-1* allele and homozygous for the rescue construct; these plants had full seed set. These data indicate that disruption of the *MYB98* gene is responsible for the female gametophyte defect in *myb98-1* mutants.

Terminal Phenotype of *myb98* Female Gametophytes

To determine whether *myb98* mutants are affected in female gametophyte development, we analyzed *myb98-1* and *myb98-2* female gametophytes at the terminal developmental stage (stage FG7) using confocal laser scanning microscopy (CLSM) (Christensen et al., 1997). Wild-type synergid cells are highly polarized, with their nuclei and most of their cytoplasm located at the micropylar pole and their vacuoles at the chalazal poles (Figures 1A, 1B, and 5A). *myb98* female gametophytes and *myb98* synergid cells in particular (Figure 5B) appeared normal at the level of CLSM, indicating that female gametophyte development and the overall morphology of the synergid cells were not largely affected by the *myb98-1* and *myb98-2* mutations.

Filiform Apparatus Structure Is Abnormal in *myb98* Synergid Cells

To determine whether *myb98* female gametophytes have defects at the ultrastructural level, we analyzed mutants using transmission electron microscopy. This analysis showed that the structure of the filiform apparatus is abnormal in *myb98* synergid cells.

In the wild type, the filiform apparatus appeared to consist of numerous finger-like projections of the cell wall into the synergid cytoplasm. This was most clearly seen in the chalazal-most region of the filiform apparatus, where individual projections could be observed (Figures 5E and 5G). In the micropylar-most region of the filiform apparatus, the structure was complex and heterogeneous (Figure 5G), suggesting that the finger-like projections are interlaced in this region. Throughout the filiform apparatus, electron-dense and electron-translucent regions were present (Figures 5G and 5I) (Willemse and van Went, 1984; Huang and Russell, 1992).

In contrast with the wild type, the cell wall at the micropylar region of *myb98* synergid cells lacked the extensive invaginations characteristic of the filiform apparatus (Figures 5F, 5H, and 5J to 5L). In place of the filiform apparatus was a structure that resembles an extremely thickened cell wall (Figures 5F, 5H, and 5K). In most of the *myb98* female gametophytes analyzed (five of five *myb98-1* and three of five *myb98-2*), this micropylar structure lacked cell wall projections completely (Figure 5J) and had uniform electron density (Figure 5H). However, in two of the *myb98-2* female gametophytes analyzed, primitive cell wall projections and electron-dense and electron-translucent regions were present (Figures 5K and 5L). In addition to the filiform apparatus defect, the cell wall between the synergid cells was thicker in the mutant than in the wild type (Figures 5E and 5F). Other aspects of synergid cell ultrastructure appeared normal in *myb98* synergid cells. Together, these data suggest that *MYB98* is required for the formation of the filiform apparatus during synergid cell differentiation.

Pollen Tube Guidance Is Defective in *myb98* Synergid Cells

Laser ablation studies have shown that the synergid cells secrete an attractant that guides the pollen tube to the female gametophyte (Higashiyama et al., 2001). To test for defects in pollen tube guidance, we pollinated *myb98-1/myb98-1* and *myb98-1/MYB98* pistils with wild-type pollen and observed pollen tubes at 12 h after pollination. In the wild type, the pollen tube grew along

Table 1. Segregation of the *myb98-1* and *myb98-2* Mutations

Parental Genotypes		Progeny Genotypes		
Male	Female	*MYB98/MYB98*	*myb98/MYB98*	*myb98/myb98*
myb98-1/MYB98	*myb98-1/MYB98*	109	113	5
MYB98/MYB98	*myb98-1/MYB98*	304	3	–
myb98-1/MYB98	*MYB98/MYB98*	160	172	–
myb98-2/MYB98	*myb98-2/MYB98*	367	388	13
MYB98/MYB98	*myb98-2/MYB98*	368	5	–
myb98-2/MYB98	*MYB98/MYB98*	187	217	–

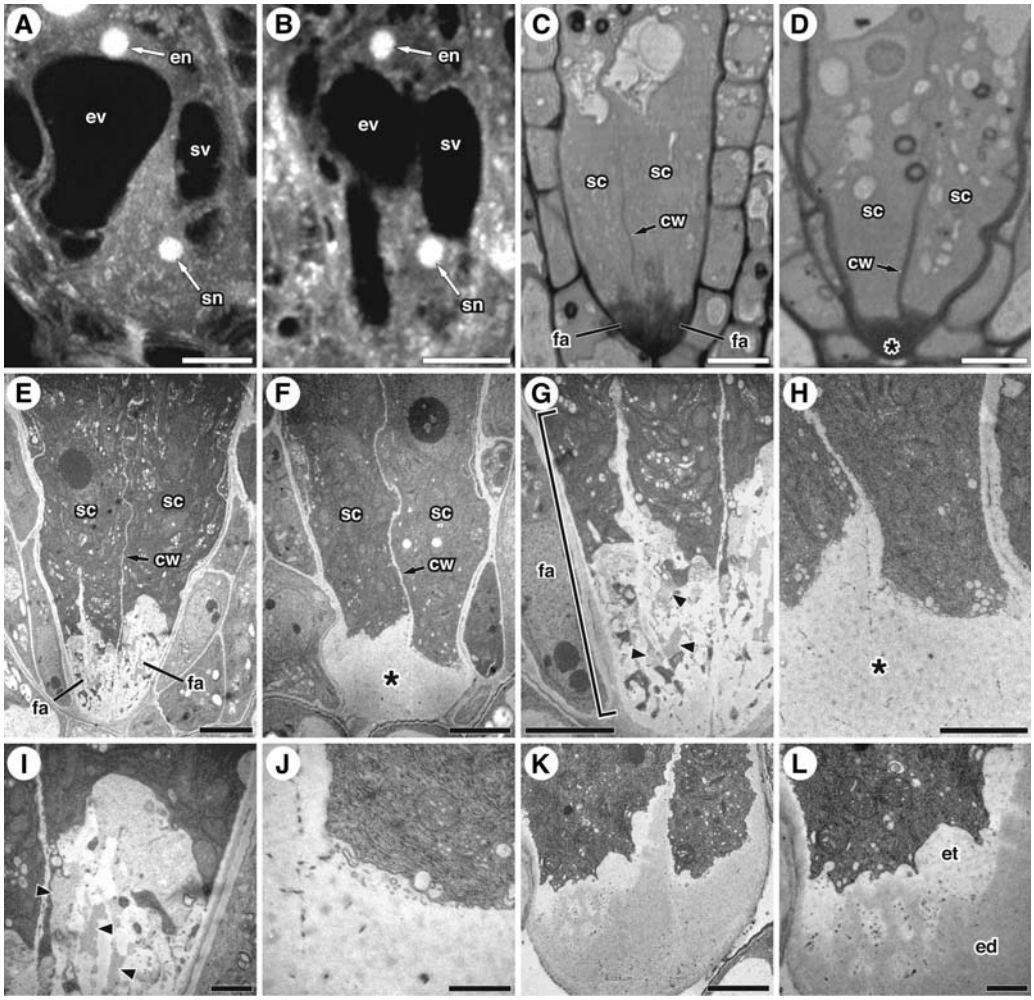

Figure 5. Microscopic Analysis of *myb98* Female Gametophytes.

(A) and **(B)** CLSM images of female gametophytes at the terminal developmental stage (stage FG7) in the wild type **(A)** and *myb98-1* **(B)**.
(C) and **(D)** Light micrographs of synergid cells from thick plastic sections of wild-type **(C)** and *myb98-1* **(D)** ovules.
(E) to **(L)** Transmission electron microscopy images of wild-type (**[E]**, **[G]**, and **[I]**), *myb98-1* (**[F]**, **[H]**, and **[J]**), and *myb98-2* (**[K]** and **[L]**) synergid cells. The asterisks in **(D)**, **(F)**, and **(H)** denote the abnormal micropylar structure in *myb98-1* synergid cells. Within the filiform apparatus of the wild type (**[G]** and **[I]**) are electron-translucent (light gray patches) and electron-dense (medium gray patches marked with arrowheads) regions. The dark gray regions are pockets of cytoplasm.
cw, cell wall between the synergid cells; ed, electron-dense region; en, egg cell nucleus; et, electron-translucent region; ev, egg cell vacuole; fa, filiform apparatus; sc, synergid cell; sn, synergid cell nucleus; sv, synergid cell vacuole. Bars = 10 μm in **(A)** and **(B)**, 5 μm in **(C)** to **(F)**, 3 μm in **(G)**, **(H)**, and **(K)**, and 1 μm in **(I)**, **(J)**, and **(L)**.

the ovule's funiculus, through the ovule's micropyle, and into the female gametophyte (Figure 6A). By contrast, wild-type pollen tubes grew abnormally on ovules containing *myb98-1* female gametophytes: pollen tubes grew from the placenta to the funiculus but then failed to grow into the micropyle (Figure 6B). Similar results were obtained with *myb98-2/MYB98* pistils. Thus, pollen tube guidance is affected in *myb98-1* and *myb98-2* female gametophytes.

We also scored pollen tube growth at 24 h after pollination. In the wild type at this time point, 98% ($n = 100$) of ovules received a single pollen tube. By contrast, multiple (≥3 per ovule) pollen tubes were present on all ($n = 200$) *myb98-1/myb98-1* ovules (Figures 6C and 6D). The majority of these were present at random positions on the ovule. However, in 20% of *myb98-1/myb98-1* ovules ($n = 100$ ovules), one of the pollen tubes had grown into the micropyle (Figure 6D); these most likely become fertilized and give rise to seeds, based on the observed 17% seed set in *myb98-1/myb98-1* mutants (discussed above).

The *myb98* Mutation Does Not Affect the Fertilization Process

Previous genetic and structural studies suggest that the synergid cells control several steps of the fertilization process, including

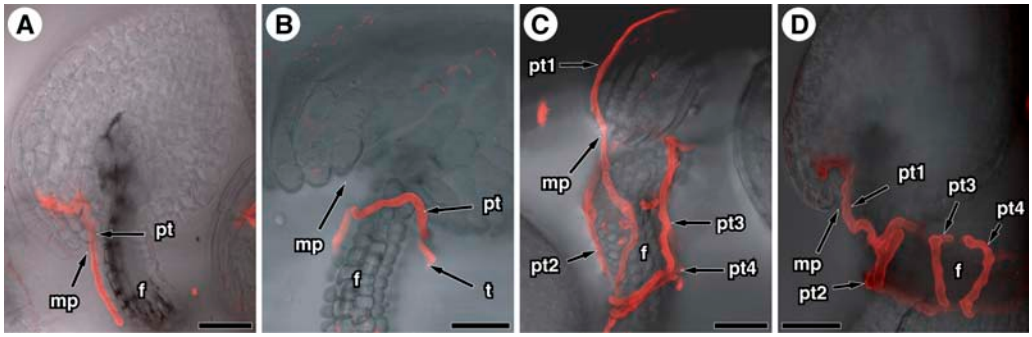

Figure 6. Pollen Tube Guidance Is Affected in *myb98* Female Gametophytes.

(A) Wild-type pollen tube on a wild-type ovule at 12 h after pollination.
(B) Wild-type pollen tube on a *myb98-1/myb98-1* ovule at 12 h after pollination.
(C) Wild-type pollen tubes on a *myb98-1/myb98-1* ovule at 24 h after pollination. Four pollen tubes (pt1 to pt4) are present on the ovule.
(D) Wild-type pollen tubes on a *myb98-1/myb98-1* ovule at 24 h after pollination. Four pollen tubes (pt1 to pt4) are present on the ovule. One of the pollen tubes (pt1) is in the micropyle.
All images are composites composed of CLSM micrographs of the pollen tubes merged with bright-field images of ovules. All images are projections of multiple 1-μm sections. f, funiculus; mp, micropyle; pt, pollen tube; t, tip of pollen tube. Bars = 25 μm.

the arrest of pollen tube growth, the release of pollen tube contents, and the migration of the sperm cells to the egg cell and central cell (Weterings and Russell, 2004). To determine whether *myb98* female gametophytes have defects in these steps of the fertilization process, we asked whether mutant female gametophytes could become fertilized and give rise to seeds if penetrated by a pollen tube. Addressing this question was made possible by the partial seed set exhibited by homozygous *myb98-1* mutants (discussed above). The partial seed set suggests either that *myb98-1* female gametophytes can function normally if penetrated by a pollen tube or that the *myb98-1* mutation is partially penetrant. To distinguish between these possibilities, we prepared and analyzed thick plastic sections (Figures 5C and 5D) of 30 *myb98-1* female gametophytes. We found that all 30 had defects in the filiform apparatus. Therefore, it is unlikely ($P < 0.003$) that the 17% seed set is attributable to partial penetrance of the *myb98-1* mutation. These data suggest very strongly that female gametophytes affected by the *myb98-1* mutation can become fertilized and give rise to seeds. Thus, with the exception of pollen tube guidance, the synergid cells appear to function normally in *myb98-1* female gametophytes.

DISCUSSION

MYB98 Is Required for Synergid Cell Differentiation

In the context of the ovule, *MYB98* is expressed exclusively in the synergid cells (Figures 3A and 3B). During female gametophyte development, *MYB98* is expressed after but not before cellularization (Figure 3C). This specialized expression pattern is consistent with the phenotype of *myb98* mutants, which are affected in pollen tube guidance and filiform apparatus structure. MYB98 likely functions as a transcription factor; thus, it is unlikely that this protein plays a direct role in pollen tube guidance and the formation of the filiform apparatus. More likely, MYB98 controls the expression of downstream genes required for these processes.

Other aspects of synergid cell development, including cell specification, appear to be normal in *myb98* mutants. This conclusion is based on several observations. First, female gametophyte development appears to be unaffected in *myb98* mutants. Second, the overall morphology of the synergid cells is unaffected in *myb98* mutants (Figures 5B and 5F). Third, the *myb98* mutation does not appear to affect steps of the fertilization process subsequent to pollen tube guidance, including the control of pollen tube growth cessation, pollen tube rupture, and sperm cell migration. Together, these observations indicate that *MYB98* controls specific aspects of synergid cell differentiation.

Expression of *MYB98* also was detected in trichomes (Figure 3G) and endosperm (Figures 3E and 3F), suggesting a function in the development of these structures. Other MYB genes play a role in trichome (Oppenheimer et al., 1991; Kirik et al., 2005; Matsui et al., 2005) and endosperm (Diaz et al., 2002; Gomez et al., 2002) development. Although we did not detect trichome and endosperm defects in *myb98* mutants, *MYB98* could function redundantly with other MYB genes.

Function of the Filiform Apparatus

During the fertilization process, the pollen tube enters the female gametophyte by growing through the filiform apparatus and into one of the synergid cells (Weterings and Russell, 2004). This growth pattern suggests that the filiform apparatus plays a role in the entry of the pollen tube into the female gametophyte. For example, it has been proposed that the filiform apparatus protects the female gametophyte from mechanical damage by restricting the pathway of pollen tube growth (Higashiyama, 2002). *myb98* embryo sacs have structural defects in the filiform apparatus but can become fertilized. These observations indicate that a fully elaborated filiform apparatus is not required for pollen tube entry into the synergid cell.

The filiform apparatus consists of numerous finger-like projections of the cell wall that extend deeply into the synergid cytoplasm (Figures 5E and 5G). The filiform apparatus greatly increases the surface area of the plasma membrane at the micropylar poles of the synergid cells. Based on these structural observations, it has been proposed that the filiform apparatus facilitates the transport of substances into and out of the synergid cells (Willemse and van Went, 1984; Huang and Russell, 1992; Higashiyama, 2002).

For example, it has been proposed that the filiform apparatus facilitates the export of a pollen tube attractant (Huang and Russell, 1992; Higashiyama, 2002). Consistent with this proposal, *myb98* female gametophytes exhibit defects in pollen tube guidance. Thus, the pollen tube guidance defect in *myb98* female gametophytes may be a secondary consequence of the filiform apparatus defect. However, at present, we cannot eliminate the possibility that *MYB98* is required for the production of a pollen tube attractant in addition to its role in filiform apparatus formation.

It also has been proposed that the filiform apparatus mediates the uptake of metabolites into the embryo sac (Jensen, 1965; Huang and Russell, 1992). If true, *myb98* female gametophytes should exhibit reduced viability as a result of nutritional deficiency. However, with the exception of the filiform apparatus defect, *myb98* embryo sacs appear structurally normal (Figures 5B and 5F). These observations suggest that the filiform apparatus does not mediate the import of essential metabolites into the female gametophyte.

Models for the Control of Pollen Tube Guidance

Based on an analysis of pollen tube growth patterns in female gametophyte mutants affected at different developmental stages, it has been proposed that the female gametophyte is necessary for pollen tube guidance at two steps: guidance from the placenta to the funiculus (funicular guidance phase), and guidance from the funiculus to the micropyle (micropylar guidance phase) (Shimizu and Okada, 2000). On ovules containing *myb98* female gametophytes, wild-type pollen tubes grow from the placenta to the funiculus but then fail to grow into the micropyle (Figure 6B). These data support the two-step hypothesis and indicate that *myb98* affects specifically the micropylar guidance phase of pollen tube guidance.

In *myb98* female gametophytes, the filiform apparatus is affected dramatically, yet the funicular guidance phase of pollen tube guidance is unaffected. These observations indicate that the funicular guidance phase does not require the filiform apparatus and suggests three possibilities. First, the funicular guidance signal could be produced by the synergid cell but exported by a filiform apparatus–independent pathway. Second, the funicular guidance signal could be produced by a different cell type within the female gametophyte. Third, the female gametophyte could stimulate changes in the surrounding sporophytic tissue that enable pollen tube growth onto the funiculus. Consistent with the third possibility, the sporophytic ovule mutant *inner no outer* has normal embryo sacs but is impaired in funicular guidance (Baker et al., 1997).

In the wild type, typically only one pollen tube grows onto each ovule (Higashiyama, 2002; Weterings and Russell, 2004). To explain this observation, it has been proposed that the pollen tube guidance cue is eliminated upon fertilization or possibly by the entry of the pollen tube into the micropyle (Higashiyama, 2002; Weterings and Russell, 2004). Ovules containing *myb98* female gametophytes generally fail to become fertilized (Figure 6B) and also attract multiple pollen tubes (Figures 6C and 6D). Thus, our observations are consistent with the proposed model.

In ~20% of *myb98-1/myb98-1* ovules, a pollen tube grows into the micropyle and fertilizes the female gametophyte. This occasional fertilization is not attributable to partial penetrance of the *myb98-1* mutation because all of 30 embryo sacs analyzed exhibited filiform apparatus defects. The occasional fertilization instead could be the result of random growth of the pollen tubes into the micropyle. The probability of random growth into the micropyle would be increased by the numerous pollen tubes that grow onto *myb98-1/myb98-1* ovules. Alternatively, *myb98-1* synergid cells could synthesize and/or secrete a reduced level of pollen tube attractant. Distinguishing between these possibilities will likely require identification of the pollen tube attractant(s).

Model for MYB98 Function

The data presented here suggest that MYB98 functions as a transcription factor within the gene regulatory network of the synergid cell and controls the expression of downstream genes required for pollen tube guidance and the formation of the filiform apparatus. Because *myb98* synergid cells are largely normal (Figures 5B and 5F), it is unlikely that *MYB98* lies at the top of the synergid cell gene regulatory hierarchy. Instead, MYB98 is most likely a midlevel transcription factor controlling a subset of the synergid cell differentiation program; that is, MYB98 appears to control a branch of the synergid cell gene regulatory network involved specifically in pollen tube guidance and the formation of the filiform apparatus.

Identification of factors necessary for the expression of *MYB98* in the synergid cell should provide insight into the gene regulatory circuitry specifying synergid cell fate, and identification and analysis of genes downstream of MYB98 should provide insight into the mechanisms that control the generation of the filiform apparatus during synergid cell differentiation and pollen tube guidance by the mature synergid cells. Such studies should ultimately lead to an understanding of the gene regulatory networks controlling the specification and differentiation of this important cell type during female gametophyte development.

METHODS

Plant Materials and Growth Conditions

Arabidopsis thaliana seeds were sterilized in 100% ethanol and germinated on plates containing 0.5× Murashige and Skoog salts (M-9274; Sigma-Aldrich), 0.05% MES, 0.5% sucrose, and 0.8% Phytagar (Life Technologies). Ten-day-old seedlings were transferred to Scott's Redi-Earth and grown under 24-h illumination.

Plant Transformation

T-DNA constructs were introduced into *Agrobacterium tumefaciens* strain LBA4404 by electroporation. *Arabidopsis* plants (ecotype Columbia) were

transformed using a modified floral dip procedure (Clough and Bent, 1998). Transformed progeny were selected by germinating surface-sterilized T1 seeds on growth medium containing antibiotics. Resistant seedlings were transplanted to soil after 10 d of growth.

Analysis of Pro_{MYB98}:*GFP* and Pro_{MYB98}:*GUS* Expression

The Pro_{MYB98}:*GFP* and Pro_{MYB98}:*GUS* constructs included 1674 bp of sequence upstream of the translational start codon and the first exon of *MYB98*. This genomic region was obtained by PCR amplification using the primers Myb98BamF (5′-GGGGATCCGCGGCGGAGATAGTGGCT-GAGAGGTGGA-3′) and Myb98BamR (5′-TCGGATCCGTGTTCTTGAT-CACGTGTGAAG-3′). These primers introduced *Bam*HI sites at each end. The resulting PCR product was cloned into pBI101.1 (Clontech) and pBI-GFP(S65T) (Choi et al., 2002) using the *Bam*HI sites, resulting in plasmids pBI101-pMYB98:GUS and pBI-pMYB98:GFP. These constructs were introduced into *Arabidopsis* plants as described above, and transformed plants were selected by germinating seeds on growth medium containing 40 μg/mL kanamycin. The expression patterns reported in Results are derived from the analysis of five single-insert Pro_{MYB98}:*GUS* lines and seven single-insert Pro_{MYB98}:*GFP* lines.

Tissue from plants containing the pBI101-pMYB98:GUS construct was stained for GUS activity in a solution containing 50 mM sodium phosphate buffer, pH 7.0, 0.2% Triton X-100, 10 mM potassium ferrocyanide, 10 mM potassium ferricyanide, and 1 mM X-Gluc. For staining of ovule tissue, flowers were emasculated at stage 12c (Christensen et al., 1997) and pistils were collected at 24 h after emasculation. Ovules were dissected from the pistil tissue, placed into staining solution on ice, vacuum-infiltrated for 15 min, and stained for 30 min at 37°C. Seeds were processed as above except for the modifications described in the legend of Figure 3. Seedlings (for analysis of expression in leaves and roots) were processed as above except that they were stained for 16 h in a solution containing 2.5 mM potassium ferrocyanide and 2.5 mM potassium ferricyanide. Flower clusters were processed as above except that they were stained for 24 h in a solution containing no potassium ferrocyanide/ferricyanide.

Tissue from plants containing the pBI-pMYB98:GFP construct was initially analyzed using an Olympus SXZ12 compound UV dissecting microscope with epifluorescence. For confocal analysis, we emasculated flowers at stage 12c, waited 24 h, and then removed the flowers from the plants. We then removed sepals, petals, and stamen and dissected off the carpel walls using a 30-gauge syringe needle. The pistils were then mounted on a slide in 10 mM phosphate buffer, pH 7.0. Pistils were analyzed using a Zeiss LSM510 confocal microscope. GFP was excited with an argon laser at a wavelength of 488 nm, and emission was detected between 500 and 530 nm.

RT-PCR

Tissue was harvested from plants and placed immediately into liquid nitrogen. Pistils were harvested from flowers at stage 13 (Smyth et al., 1990). Young flower tissue includes the inflorescence meristem and flowers at stages 1 to 11 (Smyth et al., 1990). Silique tissue includes siliques at 1 to 2 d after pollination. Leaf tissue includes leaves of 10 to 20 mm. Young leaf tissue includes the apical meristem and leaves <5 mm in length. Roots were harvested from seedlings at 10 d after germination. Floral stem tissue includes internodes from 5-week-old plants.

RNA was extracted from these tissues using the Qiagen RNeasy kit according to the manufacturer's instructions (www.qiagen.com). Aliquots of RNA (1 μg) were reverse-transcribed using the RETROscript kit (Ambion) according to the manufacturer's instructions.

For gel-based RT-PCR (Figures 2A and 2C), PCR was performed in a volume of 10 μL on a MJ PTC-200 machine. The PCR mixture consisted of 2 μL of cDNA, 1 μM primers, and 1× master mix. The PCR program consisted of a first step of denaturation and Taq activation (95°C for 4 min) followed by 30 cycles of denaturation (95°C for 5 s), annealing (60°C for 5 s), and extension (72°C for 60 s). We used primers MYB98 0ATGF (5′-CTCCTTTCCAAAACAATGGAGAATTTCGTC-3′) and MYB98 2-3 exR (5′-GTCCTCTTCTTCACTCCATGTTTCTTTCTTA-3′) for amplification of *MYB98* RNA, and primers QACT2-F (5′-TCCCTCAGCACATTCCAGCA-GAT-3′) and QACT2-R (5′-AACGATTCCTGGACCTGCCTCATC-3′) for amplification of *ACTIN2* RNA.

For real-time RT-PCR, PCR was performed using the Roche FastStart DNA Master SYBR Green I master mix (www.roche.com) in a volume of 10 μL on a Roche LightCycler system. The PCR mixture consisted of 0.015 to 0.15 μL of cDNA, 0.5 μM primers, and 1× master mix. In every real-time RT-PCR run, *ACTIN2* was used as an internal control to normalize for variation in the amount of cDNA template. The PCR primers used were qMYB98F-IH (5′-AAGACAGGGTACTGATTCAACTCG-3′) and QMYB98-R (5′-AGCGATATGCGACCATTTACGCAA-3′). The PCR program consisted of a first step of denaturation and Taq activation (95°C for 5 min) followed by 45 cycles of denaturation (95°C for 15 s), annealing (60°C for 15 s), and extension (72°C for 10 s). To determine the specificity of the PCR, the amplified products were subjected to melt curve analysis using the machine's standard method. For each gene analyzed, at least four PCR procedures were performed. The reported values are averages of four to five independent trials. We calculated relative expression levels as follows. We first determined the transcript levels of *MYB98* relative to a standard using the formula $\Delta C_T = C_T(MYB98) - C_T(ACTIN2)$. We next calculated an average ΔC_T value for each tissue. We then calculated relative expression levels using the equation $2^{-(\text{average } \Delta CT \text{ (tissue)} - \text{average } \Delta CT \text{ (pistil)})}$.

Cloning the *MYB98* cDNA

To amplify a cDNA encompassing the entire open reading frame of *MYB98*, we used primers MYB98 cDNA F (5′-CAATGGAGAATTTCGTC-GACGAGAATGG-3′) and MYB98 cDNA R (5′-CAAATCAGAGTCCAT-GAACAAAAGCATC-3′). The cDNA was cloned into the pCRII-TOPO vector using the TOPO TA cloning kit (Invitrogen), resulting in plasmid pCRII-cMYB98.

Sequence Analysis

We used pfam 17.0 (http://pfam.wustl.edu/hmmsearch.shtml) to identify protein motifs such as the Myb domains. We used psort (http://psort.nibb.ac.jp/form.html) to identify the putative nuclear localization signal. We used the MegAlign module of the DNAStar Lasergene suite to align sequences; specifically, we used the Lipman-Pearson algorithm for the alignment of protein sequences and the Wilbur-Lipman algorithm for the alignment of nucleotide sequences.

Characterization of the *myb98-1* and *myb98-2* Alleles

myb98-1 (SALK_020263) and *myb98-2* (SALK_147765) were obtained from the Salk Institute Genomic Analysis Laboratory collection (Alonso et al., 2003). The T-DNA insertion in *myb98-1* has two left borders. The T-DNA is inserted into the genomic sequence 42 nucleotides downstream of the start codon in *MYB98* and is associated with a 23-bp deletion (nucleotides +43 to +65 deleted). The left border–genomic sequence junctions were determined by PCR using the T-DNA–specific primer LBa1 (5′-TGGTTCACGTAGTGGGCCATCG-3′) combined with the genomic sequence primer Myb98-1RP (5′-TCCACTGCTTGGAAATGATGATG-3′) and the T-DNA–specific primer ROK2 6781 RC (5′-ATCGCGCGCGGTG-TCATCTA-3′) combined with the genomic sequence primer Myb98-1 LP (5′-TGTTTACCCCAAATTCAACAACACC-3′).

The T-DNA insertion in *myb98-2* has two left borders. The T-DNA is inserted into the genomic sequence 195 nucleotides upstream of the start

codon of *MYB98* and is associated with a 19-bp deletion (nucleotides −196 to −214 deleted). The left border–genomic sequence junctions were determined by PCR using the T-DNA–specific primer LBa1 (see above) combined with the genomic sequence primer Myb98-2RP (5′-GCTTGTAGGTTTTGATTGGTCG-3′) and the T-DNA–specific primer LBa1 (see above) combined with the genomic sequence primer Myb98-2 LP (5′-TTGGTCAGAGACTTTTTGTGAGGG-3′).

Segregation Analysis

Plants segregating the *myb98-1* allele were genotyped by PCR using the following primers: LBa1, Myb98-1LP, and Myb98-1RP (see above). Plants segregating the *myb98-2* allele were genotyped by PCR using the following primers: LBa1, Myb98-2LP, and Myb98-2RP (see above). Heterozygous plants, identified by PCR, were used in the segregation analysis described below.

For self cross analysis, heterozygous plants were allowed to self-pollinate and progeny seed was collected. The progeny seed was germinated on growth medium containing no antibiotics. The progeny were genotyped and scored with PCR using the primers listed above.

For reciprocal cross analysis, heterozygous plants were crossed with the wild type as outlined in Table 1 and progeny seed was collected. The F1 seed was germinated on growth medium containing 50 μg/mL kanamycin, and the number of resistant and sensitive plants was scored. Resistant and sensitive plants were scored as being genotypes *myb98*/*MYB98* and *MYB98*/*MYB98*, respectively.

Molecular Complementation

Molecular complementation was performed using a 3768-bp DNA fragment containing the *MYB98* genomic coding sequence (1490 bp) along with 1636 bp of sequence upstream of the translational start codon and 642 bp of sequence downstream of the stop codon. This DNA fragment was amplified by PCR from BAC F28A21 using primers 98ResF (5′-AGGAATTCGAGTAACGGTAACGACGGAG-3′) and 98ResR (5′-CGAAAACCGCAGATGATTTAGAATTCGG-3′). These primers introduced *Eco*RI sites at each end. The resulting PCR product was cloned into pCAMBIA1300 (CAMBIA) using the *Eco*RI sites, producing plasmid pCAMBIA1300:MYB98. pCAMBIA1300 contains a marker gene conferring resistance to hygromycin. pCAMBIA1300:MYB98 was introduced into *Arabidopsis* plants as described above, and transformed plants were selected by germinating seeds on growth medium containing 15 μg/mL hygromycin. Hygromycin-resistant plants also containing the *myb98-1* allele were identified by PCR using primers LBa1 (5′-TGGTTCACGTAGTGGGCCATCG-3′) and Myb98-1RP (5′-TCCACTGCTTGGAAATGATGATG-3′).

Plants heterozygous for the *myb98-1* allele and hemizygous for the rescue construct were crossed as females with wild-type males. The F1 seed was germinated on growth medium containing 50 μg/mL kanamycin, and the number of resistant and sensitive plants was scored. Resistant and sensitive plants were scored as being genotypes *myb98*/*MYB98* and *MYB98*/*MYB98*, respectively. We observed 178 kanamycin-resistant progeny and 302 kanamycin-sensitive progeny. To verify that kanamycin-resistant plants had the rescue construct, we performed PCR using primers pCAMLacZR(5′-CCAGCTGGCGAAAGGGGGAT-3′)andMYB98ATG800R (5′-CCGCATCGTTTATAACAAAGTGTTAACAGTG-3′) to detect the DNA fragment. Of 27 kanamycin-resistant plants analyzed, all contained the rescue construct. Three single-insert lines were analyzed.

To identify plants homozygous for both *myb98-1* and the rescue construct, we crossed plants heterozygous for *myb98-1* and hemizygous for the rescue construct with *myb98-1*/*myb98-1*. In the F2 generation, we identified plants in which 100% of the progeny were resistant to both kanamycin and hygromycin. Two plants of this genotype were identified and analyzed.

Confocal Analysis of Female Gametophyte Structure

Confocal laser scanning microscopy of ovules was performed as described previously (Christensen et al., 1997, 1998, 2002), with the modification that we used a Zeiss LSM510 microscope.

Analysis of Pollen Tube Growth

Flowers at stage 12c (Christensen et al., 1997) were emasculated and then pollinated with wild-type pollen at 24 h after emasculation. At 12 to 24 h after pollination, the flowers were removed from the plant and the sepals, petals, and stamen were removed. The carpel walls were then removed using a 30-gauge syringe needle. The resulting ovules and septum tissue were stained with 0.4% Congo red for 15 min, washed once in 0.5× Murashige and Skoog salts, and then mounted on a glass slide in 0.5× Murashige and Skoog salts. Stained pollen tubes were analyzed using a Zeiss LSM510 confocal microscope. The Congo red dye was excited with a HeNe laser at a wavelength of 543 nm. Emission was detected between 585 and 650 nm.

Plastic Sections and Transmission Electron Microscopy

Flowers from the wild type and *myb98* were emasculated at stage 12c (Christensen et al., 1997). At 24 h after emasculation, pistils were collected, cut into 1-mm pieces, and fixed overnight at 4°C in a solution of 4% glutaraldehyde, 1% paraformaldehyde, and 100 mM cacodylate buffer, pH 7.2. After fixation, the tissue was washed three times with 100 mM cacodylate buffer on ice. The tissue segments then were post-fixed for 4 h in 1% aqueous osmium tetroxide at room temperature, washed three times in distilled water, postfixed for 1 h in 1% aqueous uranyl acetate at room temperature, and washed three times in distilled water. The tissue segments then were dehydrated in a graded ethanol series (20, 40, 60, 80, 95, 95, 100, 100, and 100% for 20 min each) and then three times in propylene oxide for 10 min. The dehydrated tissues were transferred through intermediate stages of 1:2, 1:1, and 2:1 mixtures of propylene oxide:Spurr's expoxy resin and then embedded in pure Spurr's epoxy resin. The tissue blocks initially were sectioned at 1-μm thickness using an LKB Ultratome III microtome. Sections were stained with 1% toluidine blue and observed under bright-field optics using an Axioplan Zeiss microscope. For ultrastructural analysis, the same blocks were sectioned at 90-nm thickness using a Reichert-Jung Ultracut E microtome, and the sections were transferred to coated slot grids. Ultrastructural analysis was performed using a Hitachi H-7100 electron microscope at 75 kV. Images were quantified using Adobe Photoshop 7 software. Mutant and wild-type ovules were fixed in parallel.

Accession Number

The GenBank accession number for the *MYB98* Landsberg *erecta* ecotype cDNA sequence is DQ198082. The *MYB98* gene corresponds to locus At4g18770 from BAC clone F28A21 on chromosome 4.

Supplemental Data

The following material is available in the online version of this article.

Supplemental Figure 1. Comparison of *MYB98* cDNA Sequences from Ecotypes Columbia (Col) and Landsberg *erecta* (L*er*).

ACKNOWLEDGMENTS

We thank Ramin Yadegari and members of the Drews laboratory for critical review of the manuscript. We thank the ABRC for providing the *myb98* alleles. We thank Clarissa J. Christensen and Sachi Miyajima for technical assistance. We thank Ed King and the Department of Biology

Microscopy Facility for guidance with the microscopic analysis. This work was supported in part by a University of Utah Funding Incentive seed grant to G.N.D. and a USDA Cooperative State Research, Education, and Extension Service fellowship (2004-35304-14931) to M.F.P.

Received May 27, 2005; revised August 11, 2005; accepted September 14, 2005; published October 7, 2005.

REFERENCES

Acosta-Garcia, G., and Vielle-Calzada, J.P. (2004). A classical arabinogalactan protein is essential for the initiation of female gametogenesis in Arabidopsis. Plant Cell **16,** 2614–2628.

Alonso, J.M., et al. (2003). Genome-wide insertional mutagenesis of *Arabidopsis thaliana.* Science **301,** 653–657.

Bai, X., Peirson, B.N., Dong, F., Xue, C., and Makaroff, C.A. (1999). Isolation and characterization of SYN1, a RAD21-like gene essential for meiosis in Arabidopsis. Plant Cell **11,** 417–430.

Baker, S.C., Robinson-Beers, K., Villanueva, J.M., Gaiser, J.C., and Gasser, C.S. (1997). Interactions among genes regulating ovule development in *Arabidopsis thaliana.* Genetics **145,** 1109–1124.

Bhatt, A.M., Lister, C., Page, T., Fransz, P., Findlay, K., Jones, G.H., Dickinson, H.G., and Dean, C. (1999). The DIF1 gene of Arabidopsis is required for meiotic chromosome segregation and belongs to the REC8/RAD21 cohesin gene family. Plant J. **19,** 463–472.

Cai, X., Dong, F., Edelmann, R.E., and Makaroff, C.A. (2003). The Arabidopsis SYN1 cohesin protein is required for sister chromatid arm cohesion and homologous chromosome pairing. J. Cell Sci. **116,** 2999–3007.

Choi, Y., Gehring, M., Johnson, L., Hannon, M., Harada, J.J., Goldberg, R.B., Jacobsen, S.E., and Fischer, R.L. (2002). DEMETER, a DNA glycosylase domain protein, is required for endosperm gene imprinting and seed viability in Arabidopsis. Cell **110,** 33–42.

Christensen, C.A., Gorsich, S.W., Brown, R.H., Jones, L.G., Brown, J., Shaw, J.M., and Drews, G.N. (2002). Mitochondrial GFA2 is required for synergid cell death in Arabidopsis. Plant Cell **14,** 2215–2232.

Christensen, C.A., King, E.J., Jordan, J.R., and Drews, G.N. (1997). Megagametogenesis in Arabidopsis wild type and the Gf mutant. Sex. Plant Reprod. **10,** 49–64.

Christensen, C.A., Subramanian, S., and Drews, G.N. (1998). Identification of gametophytic mutations affecting female gametophyte development in Arabidopsis. Dev. Biol. **202,** 136–151.

Clough, S.J., and Bent, A.F. (1998). Floral dip: A simplified method for Agrobacterium-mediated transformation of *Arabidopsis thaliana.* Plant J. **16,** 735–743.

Cordts, S., Bantin, J., Wittich, P.E., Kranz, E., Lorz, H., and Dresselhaus, T. (2001). ZmES genes encode peptides with structural homology to defensins and are specifically expressed in the female gametophyte of maize. Plant J. **25,** 103–114.

Diaz, I., Vicente-Carbajosa, J., Abraham, Z., Martinez, M., Isabel-La Moneda, I., and Carbonero, P. (2002). The GAMYB protein from barley interacts with the DOF transcription factor BPBF and activates endosperm-specific genes during seed development. Plant J. **29,** 453–464.

Drews, G.N., Lee, D., and Christensen, C.A. (1998). Genetic analysis of female gametophyte development and function. Plant Cell **10,** 5–17.

Gomez, E., Royo, J., Guo, Y., Thompson, R., and Hueros, G. (2002). Establishment of cereal endosperm expression domains: Identification and properties of a maize transfer cell-specific transcription factor, ZmMRP-1. Plant Cell **14,** 599–610.

Higashiyama, T. (2002). The synergid cell: Attractor and acceptor of the pollen tube for double fertilization. J. Plant Res. **115,** 149–160.

Higashiyama, T., Kuroiwa, H., Kawano, S., and Kuroiwa, T. (1998). Guidance in vitro of the pollen tube to the naked embryo sac of *Torenia fournieri.* Plant Cell **10,** 2019–2032.

Higashiyama, T., Yabe, S., Sasaki, N., Nishimura, Y., Miyagishima, S., Kuroiwa, H., and Kuroiwa, T. (2001). Pollen tube attraction by the synergid cell. Science **293,** 1480–1483.

Huang, B.-Q., and Russell, S.D. (1992). Female germ unit: Organization, isolation, and function. Int. Rev. Cytol. **140,** 233–292.

Huck, N., Moore, J.M., Federer, M., and Grossniklaus, U. (2003). The Arabidopsis mutant feronia disrupts the female gametophytic control of pollen tube reception. Development **130,** 2149–2159.

Hulskamp, M., Schneitz, K., and Pruitt, R.E. (1995). Genetic evidence for a long-range activity that directs pollen tube guidance in *Arabidopsis.* Plant Cell **7,** 57–64.

Jensen, W.A. (1965). The ultrastructure and histochemistry of the synergids of cotton. Am. J. Bot. **52,** 238–256.

Jia, L., Clegg, M.T., and Jiang, T. (2004). Evolutionary dynamics of the DNA-binding domains in putative R2R3-MYB genes identified from rice subspecies indica and japonica genomes. Plant Physiol. **134,** 575–585.

Jiang, C., Gu, X., and Peterson, T. (2004). Identification of conserved gene structures and carboxy-terminal motifs in the Myb gene family of Arabidopsis and *Oryza sativa* L. ssp. *indica.* Genome Biol. **5,** R46.

Jin, H., and Martin, C. (1999). Multifunctionality and diversity within the plant MYB-gene family. Plant Mol. Biol. **41,** 577–585.

Kanei-Ishii, C., Sarai, A., Sawazaki, T., Nakagoshi, H., He, D.N., Ogata, K., Nishimura, Y., and Ishii, S. (1990). The tryptophan cluster: A hypothetical structure of the DNA-binding domain of the myb protooncogene product. J. Biol. Chem. **265,** 19990–19995.

Kirik, V., Lee, M.M., Wester, K., Herrmann, U., Zheng, Z., Oppenheimer, D., Schiefelbein, J., and Hulskamp, M. (2005). Functional diversification of MYB23 and GL1 genes in trichome morphogenesis and initiation. Development **132,** 1477–1485.

Kranz, H., Scholz, K., and Weisshaar, B. (2000). c-MYB oncogene-like genes encoding three MYB repeats occur in all major plant lineages. Plant J. **21,** 231–235.

Lipsick, J.S., and Wang, D.M. (1999). Transformation by v-Myb. Oncogene **18,** 3047–3055.

Marton, M.L., Cordts, S., Broadhvest, J., and Dresselhaus, T. (2005). Micropylar pollen tube guidance by egg apparatus 1 of maize. Science **307,** 573–576.

Matsui, K., Hiratsu, K., Koyama, T., Tanaka, H., and Ohme-Takagi, M. (2005). A chimeric AtMYB23 repressor induces hairy roots, elongation of leaves and stems, and inhibition of the deposition of mucilage on seed coats in Arabidopsis. Plant Cell Physiol. **46,** 147–155.

Ogata, K., Hojo, H., Aimoto, S., Nakai, T., Nakamura, H., Sarai, A., Ishii, S., and Nishimura, Y. (1992). Solution structure of a DNA-binding unit of Myb: A helix-turn-helix-related motif with conserved tryptophans forming a hydrophobic core. Proc. Natl. Acad. Sci. USA **89,** 6428–6432.

Ogata, K., Morikawa, S., Nakamura, H., Sekikawa, A., Inoue, T., Kanai, H., Sarai, A., Ishii, S., and Nishimura, Y. (1994). Solution structure of a specific DNA complex of the Myb DNA-binding domain with cooperative recognition helices. Cell **79,** 639–648.

Ogata, K., et al. (1995). Comparison of the free and DNA-complexed forms of the DNA-binding domain from c-Myb. Nat. Struct. Biol. **2,** 309–320.

Oppenheimer, D.G., Herman, P.L., Sivakumaran, S., Esch, J., and

Marks, M.D. (1991). A myb gene required for leaf trichome differentiation in Arabidopsis is expressed in stipules. Cell **67,** 483–493.

Ray, S., Park, S.-S., and Ray, A. (1997). Pollen tube guidance by the female gametophyte. Development **124,** 2489–2498.

Rotman, N., Rozier, F., Boavida, L., Dumas, C., Berger, F., and Faure, J.E. (2003). Female control of male gamete delivery during fertilization in *Arabidopsis thaliana.* Curr. Biol. **13,** 432–436.

Russell, S.D. (1993). The egg cell: Development and role in fertilization and early embryogenesis. Plant Cell **5,** 1349–1359.

Shimizu, K.K., and Okada, K. (2000). Attractive and repulsive interactions between female and male gametophytes in Arabidopsis pollen tube guidance. Development **127,** 4511–4518.

Smyth, D.R., Bowman, J.L., and Meyerowitz, E.M. (1990). Early flower development in Arabidopsis. Plant Cell **2,** 755–767.

Stracke, R., Werber, M., and Weisshaar, B. (2001). The R2R3-MYB gene family in *Arabidopsis thaliana.* Curr. Opin. Plant Biol. **4,** 447–456.

Tahirov, T.H., et al. (2002). Mechanism of c-Myb-C/EBP beta cooperation from separated sites on a promoter. Cell **108,** 57–70.

Weterings, K., and Russell, S.D. (2004). Experimental analysis of the fertilization process. Plant Cell **16** (suppl.), S107–S118.

Willemse, M.T.M., and van Went, J.L. (1984). The female gametophyte. In Embryology of Angiosperms, B.M. Johri, ed (Berlin: Springer-Verlag), pp. 159–196.

Williams, E.G., Kaul, V., Rouse, J.L., and Palser, B.F. (1986). Overgrowth of pollen tubes in embryo sacs of *Rhododendron* following interspecific pollinations. Aust. J. Bot. **34,** 413–423.